ELSEVIER

Clinical Neurophysiology 114 (2003) 2258–2267

www.elsevier.com/locate/clinph

# Human sleep spindle characteristics after sleep deprivation

Vera Knoblauch[a], Wim L.J. Martens[b], Anna Wirz-Justice[a], Christian Cajochen[a,*]

[a]*Centre for Chronobiology, Psychiatric University Clinic, Wilhelm Klein-Str. 27, CH-4025 Basel, Switzerland*
[b]*TEMEC Instruments B.V., Spekhofstraat 2, 6466 LZ Kerkrade, The Netherlands*

Accepted 30 June 2003

**Abstract**

**Objective**: Sleep spindles (12–15 Hz oscillations) are one of the hallmarks of the electroencephalogram (EEG) during human non-rapid eye movement (non-REM) sleep. The effect of a 40 h sleep deprivation (SD) on spindle characteristics along the antero-posterior axis was investigated.

**Methods**: EEGs during non-REM sleep in healthy young volunteers were analyzed with a new method for instantaneous spectral analysis, based on the fast time frequency transform (FTFT), which yields high-resolution spindle parameters in the combined time and frequency domain.

**Results**: FTFT revealed that after SD, mean spindle amplitude was enhanced, while spindle density was reduced. The reduction in spindle density was most prominent in the frontal derivation (Fz), while spindle amplitude was increased in all derivations except in Fz. Mean spindle frequency and its variability within a spindle were reduced after SD. When analyzed per 0.25 Hz frequency bin, amplitude was increased in the lower spindle frequency range (12–13.75 Hz), whereas density was reduced in the high spindle frequency range (13.5–14.75 Hz).

**Conclusions**: The observed reduction in spindle density after SD confirms the inverse homeostatic relationship between sleep spindles and slow waves whereas the increase in spindle amplitude and the reduction in intra-spindle frequency variability support the hypothesis of a higher level of synchronization in thalamocortical cells when homeostatic sleep pressure is enhanced.


*Keywords:* Sleep homeostasis; Fast Fourier transform; Fast time frequency transform; Topography

## 1. Introduction

Sleep spindles (transient electroencephalogram (EEG) oscillations in the 12–15 Hz range) are, besides slow waves, the hallmarks of the human EEG during non-REM sleep. The mechanism underlying these oscillations depends on the degree of hyperpolarization of thalamocortical cells. At the transition from wakefulness to sleep, the membrane potential of thalamocortical cells undergoes a progressive hyperpolarization, whereby synaptic responsiveness is reduced, and the transfer of sensory information is interrupted. When a certain hyperpolarization level is achieved, rhythmic bursts in the frequency range of sleep spindles begin to appear in neurons of the nucleus reticularis of the thalamus. These oscillations are transferred to other nuclei within the thalamus and, via thalamocortical projections, to cortical cells. Further hyperpolarization of the membrane potentials leads to oscillations in the frequency range of slow waves. The sum of these oscillations at the cortical surface is represented as sleep spindles and slow waves in the macroscopic EEG (for a review see Steriade et al., 1993; Amzica and Steriade, 1998).

Spectral analysis of the non-REM sleep EEG by means of Fast Fourier Transform (FFT) revealed frequency-specific modulation of spindle frequency activity depending on circadian phase (Dijk et al., 1997; Knoblauch et al., 2003), homeostatic sleep pressure (Borbély et al., 1981; Dijk et al., 1987, 1993; Knoblauch et al., 2002), pharmacological intervention (Borbély et al., 1985; Trachsel et al., 1990; Brunner et al., 1991), and the scalp location of EEG leads (Scheuler et al., 1990; Werth et al., 1997). Here, we focus on the effect of enhanced homeostatic sleep pressure after sleep deprivation (SD) on spindle frequency activity and characteristics along the antero-posterior axis. In previous reports, spindle frequency activity was reduced in the recovery night after SD (Borbély et al., 1981;

* Corresponding author. Tel.: +41-61-325-53-18; fax: +41-61-325-55-77.
*E-mail address:* christian.cajochen@pukbasel.ch (C. Cajochen).

1388-2457/$30.00 
doi:10.1016/S1388-2457(03)00238-4

Dijk et al., 1993; Knoblauch et al., 2002) and exhibited an increasing trend across non-REM sleep episodes in the course of a night (Dijk et al., 1993; Aeschbach and Borbély, 1993; Werth et al., 1997). These results indicate an inverse homeostatic regulation of slow wave and spindle activity. The reduction of spindle frequency activity after SD was limited to the higher spindle frequency range, whereas power density in the lower spindle frequency range was not significantly affected (Borbély et al., 1981; Dijk et al., 1993) or enhanced (Knoblauch et al., 2002). It is not known whether this frequency-specific effect in the power spectra is caused by a general slowing in the spindle frequency range, which would shift the spindle frequency peak towards lower frequencies, or if it represents a frequency-specific change in the amplitude, i.e. an increase in the amplitude of low-frequency spindles and a decrease in the amplitude of high-frequency spindles. These questions cannot be *fully* answered by spectral analysis since spectral components over the considered time-window are averaged and therefore, the mean amplitude and the number of waves within the time-window cannot be segregated. Moreover, spectral analysis does not separate synchronized spindle activity from background activity in the same frequency band.

To answer these questions, data from a 40 h SD experiment, from which FFT results from the first 10 subjects have previously been reported (Knoblauch et al., 2002), were re-analyzed with a new method, the fast time frequency transform (FTFT). This method discriminates synchronized activity from background noise and calculates amplitude and incidence of synchronized spindle frequency activity with a high frequency (0.25 Hz) and temporal (0.125 s) resolution, as well as yielding a series of other spindle parameters. The aim of the present analysis was to separate and quantify the relative contribution of spindle amplitude, frequency, incidence and duration to the change in EEG power spectra after SD.

The impact of SD on sleep spindles has been studied before using methods other than spectral analysis. Spindle density, detected visually (De Gennaro et al., 2000a,b) or by transient pattern recognition (Dijk et al., 1993), was reduced after SD. The latter method calculated a number of other spindle parameters and revealed no significant change in spindle amplitude and frequency after SD. In contrast to these studies, we report regional differences in spindle incidence and amplitude after SD on a high frequency (0.25 Hz) and time (0.125 s) resolution.

## 2. Methods

### 2.1. Study participants

Sixteen healthy volunteers (8 females, 8 males, age range 20–31 years, mean: 25.3 ± 0.9 s.e.m.) participated in the study. All participants were non-smokers, free from medical, psychiatric and sleep disorders as assessed by screening questionnaires, a physical examination and a polysomnographically recorded screening night. Drug-free status was verified via urinary toxicologic analysis. Female participants were studied during the follicular phase of their menstrual cycle; 4 of them used oral contraceptives. All participants gave signed informed consent. The study protocol, screening questionnaires and consent form were approved by the local Ethical Committee, and all procedures conformed with the Declaration of Helsinki.

### 2.2. Study design

The entire study comprised two protocol blocks, a SD and a nap block, in a balanced crossover design with an off-protocol episode of 2–4 weeks in between. Here, we report data from the SD block; data from the nap block have been published elsewhere (Knoblauch et al., 2002, 2003). Volunteers reported to the laboratory in the evening and spent an 8 h night at their habitual bedtime. The timing of their sleep–wake schedule was calculated such that the 8 h sleep episode was centered at the midpoint of each volunteer's habitual sleep episode as assessed by actigraphy during the baseline week. After a second 8 h sleep episode (baseline night) at their habitual bedtime, either a 40 h SD (under constant routine conditions) or a 40 h multiple nap protocol was carried out (for details see Cajochen et al., 2001). Each study block ended with an 8 h recovery sleep episode starting again at habitual bedtime.

### 2.3. Sleep recordings and analysis

Sleep was recorded polysomnographically using the VITAPORT digital ambulatory sleep recorder (Vitaport-3 digital recorder, TEMEC Instruments B.V., Kerkrade, The Netherlands). Twelve EEGs, two electrooculograms (EOG), one submental electromyogram (EMG) and one electrocardiogram (ECG) signal were recorded. All signals were filtered at 30 Hz (4th order Bessel type anti-aliasing low-pass filter, total 24 dB/Oct.), and a time constant of 1.0 s was used prior to on-line digitization (range 610 μV, 12 bit AD converter, 0.15 μV/bit; sampling rate at 128 Hz for the EEG). The raw signals were stored on-line on a Flash RAM Card (Viking, USA) and downloaded off-line to a PC hard drive. Sleep stages were visually scored on a 20 s basis (Vitaport Paperless Sleep Scoring Software) from the C3 derivation according to standard criteria (Rechtschaffen and Kales, 1968).

### 2.4. EEG spectral analysis

EEGs were subjected to spectral analysis using an FFT (10% cosine 4 s window) resulting in a 0.25 Hz bin resolution. EEG artifacts were detected by an automated artifact detection algorithm. This algorithm was based on an instantaneous frequency analysis, which yields the amplitude-envelope and the frequency of 8 band-filtered

components instantaneously at a rate of 8 per second. Low-frequency (as movement) artifacts, mid-frequency (as ECG interference) and high-frequency (as EMG) artifacts are detected individually if the respective instantaneous frequencies and amplitudes in the relevant frequency bands are not within preset ranges (CASA, 2000 Phy Vision B.V., Kerkrade, The Netherlands). For final data reduction, the artifact-free 4 s epochs were averaged over 20 s epochs.

EEG power spectra were calculated during non-REM sleep in the frequency range between 0.5 and 32 Hz from the midline derivations (Fz, Cz, Pz, Oz) referenced against linked mastoids (A1, A2). Over the range of 0.5–25 Hz, mean EEG spectra averaged over the entire group of 16 participants were very similar to those of the first 10 participants previously published (Knoblauch et al., 2002).

### 2.5. Instantaneous spectral analysis of the EEG

The same digitized EEGs were subjected to instantaneous spectral analysis using the FTFT (Martens, 1992). For the EEG, the FTFT calculates instantaneous amplitude, frequency and bandwidth in 8 frequency bands, 0–4, 4–8,…,28–32 Hz. Instantaneous bandwidth is computed from the instantaneous frequency as the rectified first derivative with respect to time. Therefore, the higher the frequency variability, the higher the bandwidth. Based on the 4 Hz range of the filters, the temporal resolution of the above parameters is 0.125 s. Over a moving template of 1 s duration, thresholds are applied to amplitude, frequency and bandwidth parameters to differentiate synchronized activity from ongoing noise as well as to remove artifacts (Martens, 1999). The thresholds were determined empirically on a learning set of EEG recordings to yield the closest possible agreement with visual scores. Incorporating the instantaneous bandwidth helped to achieve a closer agreement than using only an amplitude threshold. Finally, the optimized settings from the learning set were applied to this data set, focusing on detected synchronized spindle activity. Spindles were detected from the outcome of the 8–12 and 12–16 Hz frequency band, but the frequency and bandwidth threshold for spindle detection was limited to the range of 11–16 Hz. These thresholds again were determined empirically and compared with visual scores. Furthermore, a duration limit ($\geq$ 0.5 and $\leq$ 2 s) was applied to detected spindles. As a result, we obtained the amplitude and frequency of each individual spindle at a time-resolution of 0.125 s and a frequency resolution of 0.25 Hz. In other words, for each 0.25 Hz frequency bin between 11 and 16 Hz, the time incidence (corresponds to the number of 0.125 s epochs within the given frequency bin) and the amplitude in these 0.125 s epochs were calculated. A further parameter was spindle density (number of sleep spindles/20 s epoch). Finally, for each individual spindle, the following parameters were computed: duration, mean frequency, mean amplitude, and standard deviation of frequency.

### 2.6. Statistics

The statistical packages SAS® (SAS® Institute Inc., Cary, NC, USA, Version 6.12) and Statistica® (StatSoft Inc. 2000. STATISTICA for Windows, Tulsa, OK, USA) were used. One-, two- and 3-way analysis of variance for repeated measures (rANOVA) were performed between the factors 'derivation' (Fz, Cz, Pz, Oz), 'night' (baseline, recovery), 'frequency bin' (12–15.5 Hz), and 'non-REM sleep episode' (non-REM sleep episode 1–4). All $p$ values derived from rANOVAs were based on Huynh–Feldt's (H–F) corrected degrees of freedom, but the original degrees of freedom are reported. For post hoc comparisons, the Duncan's multiple range test was used.

One subject was excluded from time course analysis because EEG recordings during non-REM sleep episode 3 and 4 contained considerable artifacts.

For EEG power density, spindle amplitude per 0.25 Hz and time incidence per 0.25 Hz in the range between 11 and 16 Hz (Fig. 1), a 3-way rANOVA with the factors 'derivation', 'night' and 'frequency bin' was performed and yielded a significant interaction between these 3 factors for EEG power density and time incidence, but not for amplitude. The non-significant interaction for spindle amplitude was presumably due to the prominent peak around 11.25–11.5 Hz. Because of the relatively broad frequency range for spindle detection (11–16 Hz) in the present analysis, this peak probably came about by short alpha intrusions. The rANOVA was therefore limited to a more restricted frequency range, between 12 and 15.5 Hz.

## 3. Results

### 3.1. Visual scoring

Table 1 summarizes sleep variables derived from visual scoring for the baseline night and the recovery night after SD. All variables differed significantly between the baseline and recovery night, except for REM sleep duration (percent of total sleep time) and latency to REM sleep (log-transformed; for statistics see Table 1).

### 3.2. EEG power density, spindle amplitude and time incidence per 0.25 Hz bin

In Fig. 1, EEG power density derived from spectral analysis (top panels) is illustrated along with the results from the FTFT, i.e. spindle amplitude and time incidence per 0.25 Hz bin (middle and bottom panels, respectively), from the midline derivations during baseline and recovery sleep. Values are depicted from 11 to 16 Hz, statistics was performed on the 12–15.5 Hz range (see Section 2). A 3-way rANOVA with the factors 'derivation', 'night' and 'frequency bin' yielded a significant interaction between

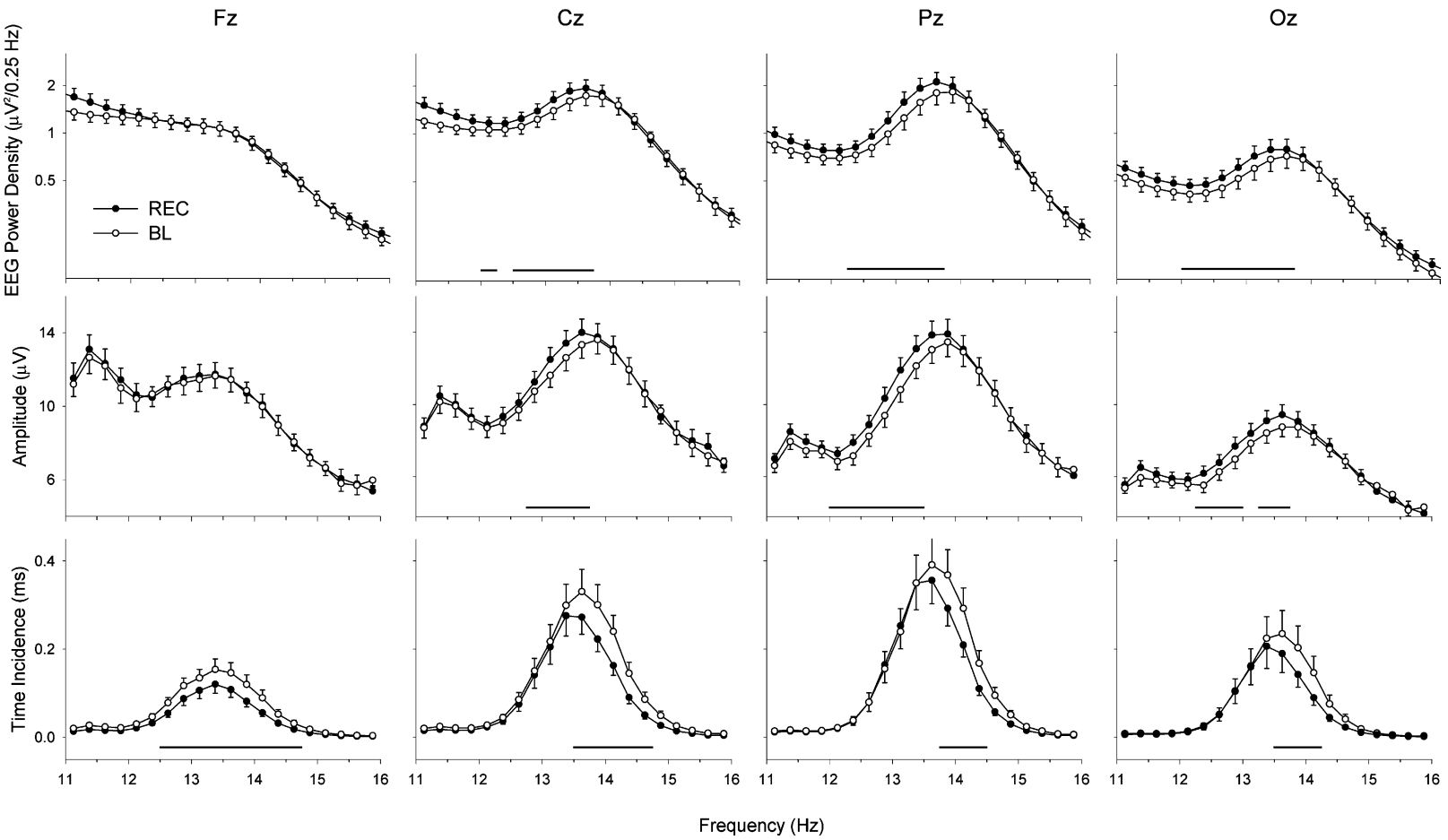


Fig. 1. EEG power density (from FFT, top panels), amplitude (from FTFT, middle panels) and frequency incidence (from FTFT, bottom panels) per 0.25 Hz bin between 11 and 16 Hz for the midline derivations (Fz, Cz, Pz, Oz) during baseline night (BL, ○) and recovery night after SD (REC, •) (mean ± s.e.m.; $n = 16$). Horizontal lines near the abscissa indicate frequency bins for which a significant difference between BL and REC was found ($p < 0.05$, Duncan's multiple range test).

Table 1
Sleep variables derived from visual scoring for the baseline and recovery night (mean ± s.e.m., $n = 16$)

| | Baseline | Recovery | |
|---|---|---|---|
| TST (min) | 438.13 ± 7.17 | 458.79 ± 3.38 | ** |
| SE (%) | 91.31 ± 1.50 | 95.72 ± 0.69 | ** |
| % MT | 3.04 ± 0.39 | 2.53 ± 0.42 | ** |
| % WALO | 6.94 ± 1.68 | 2.19 ± 0.54 | ** |
| % Stage 1 | 12.55 ± 1.41 | 6.50 ± 0.77 | ** |
| % Stage 2 | 50.25 ± 1.33 | 46.53 ± 1.19 | ** |
| % Stage 3 | 10.34 ± 0.65 | 13.66 ± 1.24 | * |
| % Stage 4 | 6.88 ± 1.46 | 14.27 ± 2.04 | ** |
| % SWS | 17.22 ± 1.65 | 27.93 ± 1.59 | ** |
| % Non-REM sleep | 67.48 ± 1.50 | 74.45 ± 1.09 | ** |
| % REM sleep | 19.97 ± 1.03 | 19.06 ± 1.22 | |
| SL1 (min) | 10.23 ± 2.25 | 3.94 ± 0.59 | ** |
| SL2 (min) | 15.19 ± 2.33 | 6.33 ± 0.75 | ** |
| RL (min) | 78.88 ± 5.95 | 73.60 ± 8.69 | |

Sleep stages are expressed as percent of total sleep time. TST, total sleep time (stage 1–4 + REM sleep); SE, sleep efficiency [(TST/time in bed)100]; MT, movement time; WALO, wakefulness after lights off; SL1, latency to stage one (min); SL2, latency to stage two (min); RL, latency to REM sleep (min). For SL1, SL2 and RL, statistics were applied on log-transformed values. Asterisks indicate significant differences between the baseline and recovery night (*$p < 0.05$, **$p < 0.01$, one-way rANOVA).

these 3 factors for EEG power density, amplitude, and time incidence (for statistics see Table 2).

### 3.3. Spectral analysis (FFT): EEG power density

EEG power density was significantly increased after SD in the lower spindle frequency range in Cz (12–12.25, 12.5–13.75 Hz), Pz (12.25–13.75 Hz ), and Oz (12–13.75 Hz; Fig. 1, top panels; $p < 0.05$, Duncan's multiple range test on log-transformed values), whereas for Fz no such difference in the 12–15.5 Hz range was found (Fig. 1, top left-hand panel).

### 3.4. Instantaneous frequency analysis (FTFT)

#### 3.4.1. Amplitude per 0.25 Hz frequency bin

Similar to EEG power density, the amplitude of synchronized spindle frequency activity per 0.25 Hz bin was increased in the low- and middle spindle frequency range after SD in Cz, Pz and Oz, but not in Fz (Fig. 1, middle panels). The increase was significant between 12.75 and 13.75 Hz in Cz, between 12 and 13.5 Hz in Pz and between 12.25 and 13 Hz and 13.25 and 13.75 Hz in Oz ($p < 0.05$, Duncan's multiple range test on log-transformed values). In addition, there was another prominent peak in the very low-frequency range, between 11.25 and 11.5 Hz.

#### 3.4.2. Time incidence per 0.25 Hz frequency bin

In contrast to EEG power density and spindle amplitude, time incidence per 0.25 Hz bin in Cz, Pz and Oz was significantly reduced in the higher spindle frequency range after SD, and not significantly changed in the lower spindle frequency range (Fig. 1, bottom panels). The reduction was significant between 13.5 and 14.75 Hz in Cz, between 13.75 and 14.5 Hz in Pz, and between 13.5 and 14.25 Hz in Oz ($p < 0.05$, Duncan's multiple range test). Time incidence in the lower and middle frequency range (up to 13.5 Hz) was not significantly changed in these derivations. In Fz, time incidence was reduced over a broader frequency range (significant between 12.5 and 14.75 Hz).

### 3.5. Spindle parameters (FTFT)

In a next step, spindle density (number per 20 s epoch), amplitude, frequency, duration, and intra-spindle frequency variability (standard deviation of intra-spindle frequency) were calculated (Fig. 2). A two-way rANOVA with the factors 'derivation' and 'night' was performed and revealed a significant effect of 'derivation' for all parameters, and a significant effect of 'night' for all parameters except for spindle duration ($p = 0.07$). The interaction between 'derivation' and 'night' was significant for spindle density, amplitude, frequency, and intra-spindle frequency variability ($p < 0.05$; two-way rANOVA). For those parameters with a significant interaction, post hoc comparison between baseline and recovery night revealed that in the recovery night, spindle density, spindle frequency, and intra-spindle frequency variability were significantly reduced in all 4 derivations, whereas spindle amplitude was significantly increased in all derivations except in Fz ($p < 0.05$;

Table 2
Three-way rANOVA with the factors derivation (D), night (N) and frequency bin (FB) for EEG power density, spindle amplitude and time incidence per 0.25 Hz frequency bin from 12–15.5 Hz ($F$; $p$)

| | | FFT power spectra | FTFT amplitude | FTFT time incidence |
|---|---|---|---|---|
| Derivation | $F$[3,45] | 70.0; <0.001 | 67.8; <0.001 | 35.6; <0.001 |
| Night | $F$[1,15] | 8.5; <0.05 | 7.3; <0.05 | 28.9; <0.001 |
| Frequency bin | $F$[13,195] | 42.4; <0.001 | 42.9; <0.001 | 23.3; <0.001 |
| D × N | $F$[3,45] | 6.6; <0.01 | 6.1; <0.01 | 3.4; <0.05 |
| D × FB | $F$[39,585] | 38.7; <0.001 | 32.6; <0.001 | 15.8; <0.001 |
| N × FB | $F$[13,195] | 2.1; 0.15 | 1.7; 0.20 | 2.6; 0.11 |
| D × N × FB | $F$[39,585] | 7.7; <0.001 | 1.9; <0.05 | 3.0; <0.05 |

For EEG power density and spindle amplitude, statistics were performed on log-transformed values.

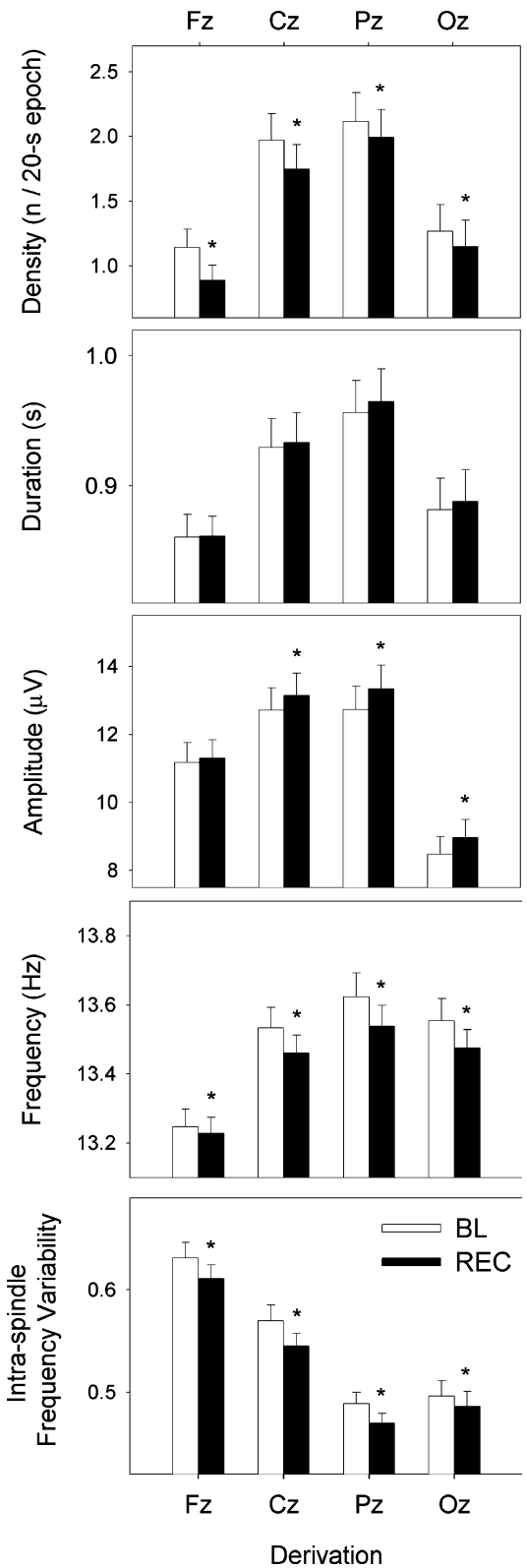


Fig. 2. Mean density (number of sleep spindles per 20 s epoch), frequency, duration, amplitude, and intra-spindle frequency variability (standard deviation of intra-spindle frequency) of sleep spindles along the midline during baseline night (BL, white bars) and recovery night after SD (REC, black bars) (mean ± s.e.m.; $n = 16$). Asterisks indicate a significant difference between BL and REC ($p < 0.05$; one-way rANOVA).

Duncan's multiple range test). In both nights, spindle density and amplitude were highest in Cz and Pz. Additionally, spindle density was significantly higher in Pz than in Cz in both nights, and spindle amplitude was significantly higher in Pz than in Cz in the recovery night, but not in the baseline night. In both nights, spindle frequency significantly increased from Fz to Cz to Pz and significantly decreased to Oz, and intra-spindle frequency variability significantly decreased from Fz to Cz to Pz, and significantly increased from Pz to Oz ($p < 0.05$; Duncan's multiple range test).

For spindle duration, the interaction between the factors 'derivation' and 'night' was not significant. When averaged across derivations, a one-way rANOVA with the factor 'night' revealed that spindle duration tended to be longer in the recovery night than in the baseline night ($p = 0.07$, one-way rANOVA).

### *3.6. Dynamics of spindle parameters across non-REM sleep episodes*

The same spindle parameters were calculated per non-REM sleep episodes (Fig. 3). A 3-way rANOVA with the factor 'derivation', 'night' and 'non-REM sleep episode' revealed no significant interaction between these 3 factors except for spindle density ($F[9, 126] = 3.54$; $p = 0.002$). For sake of clarity, only data from Fz and Pz are reported in the following.

#### *3.6.1. Baseline night*

A one-way rANOVA with the factor 'non-REM sleep episode' was performed on these parameters during the baseline night for Fz and Pz separately. All parameters derived from Pz varied significantly across non-REM sleep episodes ($F[3, 42]$ at least $> 9$; $p$ at least $< 0.001$). In Pz, spindle density and duration progressively rose over consecutive sleep episodes ($p < 0.05$; Duncan's multiple range test), and also spindle amplitude exhibited an increasing trend. An orthogonal-polynomial rANOVA yielded a significant linear component for the above parameters ($p$ at least $< 0.0001$). This linear increase was significant between non-REM sleep episode 1 and 2 and between non-REM sleep episode 2 and 4. Spindle frequency showed a U-shaped time course, which was corroborated by a significant quadratic component in the rANOVA ($F[1, 14] = 40.5$, $p < 0.0001$). It significantly decreased from a highest level in non-REM episode 1 to non-REM episode 2 and increased from non-REM episode 3 to 4. Intra-spindle frequency variability was highest at the beginning of the night and significantly declined from episode 1 to 2 ($p < 0.05$, Duncan's multiple range test), and both a significant linear and quadratic component were present ($p$ at least $< 0.001$). In contrast to Pz, spindle amplitude and spindle frequency in Fz remained fairly stable and did not show a significant variation across non-REM sleep episodes ($p$ at least $> 0.16$). The other spindle

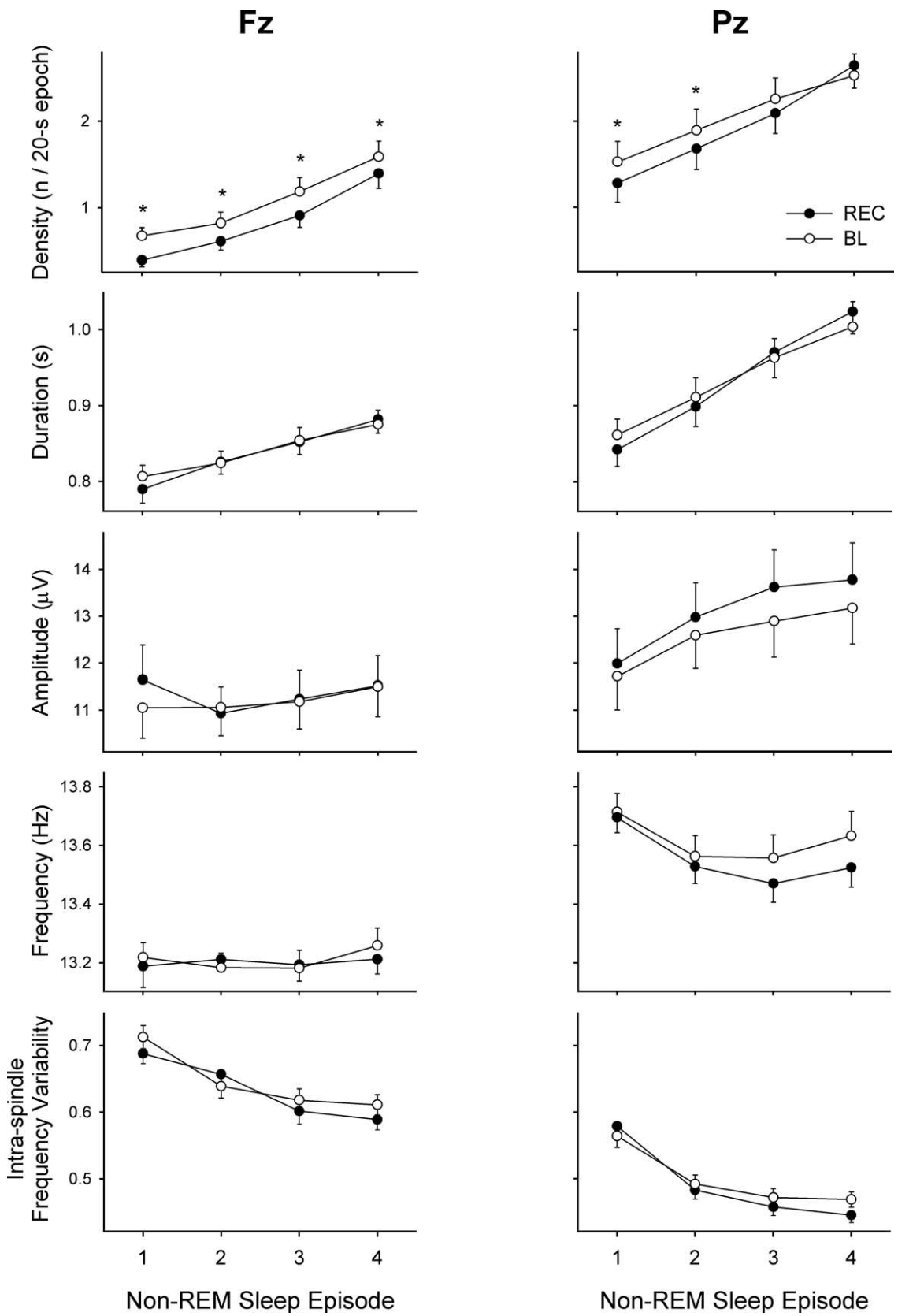


Fig. 3. Mean spindle density (number of sleep spindles per 20 s epoch), frequency, duration, amplitude, and intra-spindle frequency variability (standard deviation of intra-spindle frequency) in Fz and Pz during non-REM sleep episodes of the baseline (BL, ○) and recovery night (REC, •) (mean ± s.e.m.; $n = 15$). Asterisks indicate significant differences to corresponding baseline values ($p < 0.05$, Duncan's multiple range test).

parameters such as spindle density, duration and intra-spindle frequency variability showed similar time courses in Fz as for Pz, but on different absolute levels (compare left and right-hand side panels in Fig. 3).

*3.6.2. Effect of SD*

To assess whether the time course of spindle parameters in Fz and Pz was changed after SD, a two-way rANOVA with the factors 'non-REM sleep episode' and 'night' was performed for Fz and Pz separately. For Pz, the factor 'non-REM sleep episode' was significant for all parameters ($p < 0.05$). The interaction between factors 'non-REM sleep episode' and 'night' was significant for spindle density ($p < 0.05$) and tended to be significant for intra-spindle frequency variability ($p < 0.06$, two-way rANOVA; Fig. 3), indicating that SD affected the time course of these parameters. Post hoc comparison revealed that compared to the baseline night, spindle density in the recovery night was significantly reduced in episode 1 and 2 ($p < 0.05$) and tended to be reduced in episode 3 ($p = 0.06$; Duncan's multiple range test). There was no significant interaction between 'night' and 'non-REM sleep episode' for the other parameters. The factor 'non-REM sleep episode' yielded a significant main effect on all spindle parameters derived from Pz. For none of the parameters derived from Fz a significant interaction between the factors 'non-REM sleep episode' and 'night' was found ($p$ at least $> 0.1$). This indicates that, in contrast to Pz, the time course of spindle parameters derived from Fz was not significantly affected by SD. There was only a significant main effect of the factor 'night' for sleep spindle density, and a significant main effect of the factor 'non-REM episode' for spindle density, spindle duration and intra-spindle variability.

## 4. Discussion

The present data confirm and further extend that sleep spindle characteristics are significantly affected by the sleep homeostat. High-resolution analysis of spindle amplitude per 0.25 Hz bin revealed that the amplitude of sleep spindles was enhanced in the lower spindle frequency range and not affected in the high-frequency range in the recovery night after SD. In contrast, the incidence of sleep spindle activity per 0.25 Hz was reduced in the high spindle frequency range, and unchanged in the lower spindle frequency range. Our results confirm previous reports of reduced sleep spindle density after SD (Dijk et al., 1993; De Gennaro et al., 2000a). In contrast to a previous report which found no change in spindle frequency after SD using another methodology (Dijk et al., 1993), here spindle frequency was significantly reduced after SD. Within a spindle, frequency variability was reduced after SD, indicating that spindles were more homogenous and stable. The topographical analysis showed that intra-spindle frequency variability was highest in Fz and decreased from Fz to Pz. Since alpha activity exhibits a frontal predominance during non-REM sleep (Finelli et al., 2001a,b; for a review see Pivik and Harman, 1995), and the relatively broad frequency range for spindle detection (11–16 Hz) in the present analysis partly overlaps with the alpha band, the high-frequency variability in Fz was probably due to short alpha intrusions into sleep spindles. The peak between 11.25 and 11.5 Hz in spindle amplitude in Fig. 1 (middle panels, spindle amplitude per 0.25 Hz), which was most prominent in Fz, supports this hypothesis.

Also the extent of the SD effect varied between derivations, as indicated by the significant interaction between 'derivation' and 'night' for spindle density, amplitude, frequency, and intra-spindle frequency variability. In particular, the reduction in spindle density was most prominent in Fz, while spindle amplitude was increased in all derivations except in Fz. In view of the mutual exclusivity of spindle and slow wave oscillations on the level of single neurons (Nuñez et al., 1992) and on the level of the EEG (De Gennaro et al., 2000a,b; Uchida et al., 1991), this finding fits with the frontal predominance of the slow wave activity (SWA, EEG power density in the 0.75–4.5 Hz range) increase after SD (Cajochen et al., 1999).

It has been shown before that frontal spindles have a lower frequency (around 12 Hz) than parietal spindles (around 14 Hz), and these findings were interpreted as indication for the existence of two separate sleep spindle types (Gibbs and Gibbs, 1950; Zeitlhofer et al., 1997; Werth et al., 1997; Zygierewicz et al., 1999; Anderer et al., 2001). Our data do not corroborate such a concept that frontally and parietally scalp-recorded sleep spindles originate from two functionally distinct thalamic sources. We think that differences between frontally and parietally scalp-recorded sleep spindles rather represent a topography-dependent modulation of one single type of spindle oscillations, whose origin can be traced back to the thalamic reticular nucleus from where it disseminates to distant sites within the thalamus.

The reduction in spindle density, most pronounced in the first part of the night, confirms the expected and previously described inverse relationship to slow waves (Borbély et al., 1981; Dijk et al., 1993; Finelli et al., 2001a). This reciprocity between slow waves and sleep spindles is based on their generating mechanism at the cellular level. After sleep onset, the progressive hyperpolarization in thalamic and cortical neurons leads to oscillations in the membrane potential in the frequency range of spindles, and, with further hyperpolarization, in the frequency range of delta waves (for a review see Amzica and Steriade, 1998). When sleep pressure is high, this hyperpolarization seems to proceed faster. The more rapid rise of both spindle and slow wave activity in the first minutes of recovery sleep after SD (Dijk et al., 1993) supports this hypothesis. Since the degree of hyperpolarization is enhanced after SD, more neurons would fire in the delta instead of the spindle mode. This would explain the reduction of spindle density after SD.

The reduction in spindle density is not contradictory to the enhanced spindle amplitude seen after SD. The above described oscillations in thalamic and cortical neurons are only reflected in the scalp-recorded EEG when a large number of neurons synchronously oscillate in these frequency modes. With sleep deepening, larger numbers of neurons are recruited to oscillate in the spindle or delta mode, and their firing activity becomes more synchronized. Thus, while wakefulness is characterized by low-amplitude oscillations of relatively low spatio-temporal coherence, oscillations during sleep exhibit high temporal and spatial correlation across wide regions of the cortex (Sejnowski and Destexhe, 2000). The size of the neuronal population that oscillates in synchrony with a given frequency, is, on the level of the macroscopic EEG, reflected in the amplitude of the wave with this frequency (Amzica and Steriade, 1998). Both the increase of SWA (Borbély et al., 1981; Dijk et al., 1993; Finelli et al., 2001b; Knoblauch et al., 2002) and the reported increase here in spindle amplitude indicate that the recruitment of large neuronal populations and their synchronization is reinforced after SD. The reduction in intra-spindle frequency variability also supports this hypothesis of a higher level of synchronization of thalamic and cortical oscillations under high sleep pressure.

Mean spindle frequency was reduced after SD. Our data indicate that a specific reduction in the incidence of fast spindle components, rather than a uniform slowing of spindles, underlies the frequency reduction. The reduction in the incidence of high-frequency spindle elements calculated by the FTFT was not manifested in the FFT power spectrum. This suggests that the power spectrum mainly represents changes in spindle amplitude, while changes in spindle frequency and incidence are poorly reflected. Additionally, the fact that FFT power spectra include background activity within the spindle frequency range, while spindle FTFT discriminates synchronized spindle activity from background noise, may also contribute to the discrepancy between the results from the two methods.

Taken together, non-REM sleep EEGs from the recovery night after a 40 h SD were analyzed with two methods, the classical spectral analysis by means of FFT, and the new instantaneous spectral analysis by means of FTFT. Whereas the effect of SD on EEG power density in the spindle frequency range has been described before (Borbély et al., 1981; Dijk et al., 1993; Finelli et al., 2001a,b; Knoblauch et al., 2002), the present results from the FTFT provide additional, more detailed information about the changes sleep spindles undergo when homeostatic sleep pressure is enhanced, and thereby contribute to a more comprehensive understanding of the homeostatic regulation of sleep spindles. The increase in spindle amplitude and the decrease in intra-spindle frequency variability support the hypothesis of a higher degree of synchronization of oscillations in cortico-thalamic circuitries under enhanced sleep pressure.

## Acknowledgements

We thank Claudia Renz, Giovanni Balestrieri and Marie-France Dattler for their help in data acquisition, Drs. Alexander Rösler and Tobias Müller for medical screenings, and the subjects for participating. This research was supported by Swiss National Foundation Grants START #3130-054991.98 and #3100-055385.98 to CC.

## References

Aeschbach D, Borbély AA. All-night dynamics of the human sleep EEG. J Sleep Res 1993;2:70–81.

Amzica F, Steriade M. Electrophysiological correlates of sleep delta waves. Electroenceph clin Neurophysiol 1998;107:69–83.

Anderer P, Klösch G, Gruber G, Trenker E, Pascual-Marqui RD, Zeitlhofer J, et al. Low-resolution brain electromagnetic tomography revealed simultaneously active frontal and parietal sleep spindle sources in the human cortex. Neuroscience 2001;103:581–92.

Borbély AA, Baumann F, Brandeis D, Strauch I, Lehmann D. Sleep deprivation: effect on sleep stages and EEG power density in man. Electroenceph clin Neurophysiol 1981;51:483–95.

Borbély AA, Mattmann P, Loepfe M, Strauch I, Lehmann D. Effect of benzodiazepine hypnotics on all-night sleep EEG spectra. Hum Neurobiol 1985;4:189–94.

Brunner DP, Dijk DJ, Münch M, Borbèly AA. Effect of zolpidem on sleep and sleep EEG spectra in healthy young men. Psychopharmacology 1991;104:1–5.

Cajochen C, Foy R, Dijk DJ. Frontal predominance of a relative increase in sleep delta and theta EEG activity after sleep loss in humans. Sleep Res Online 1999;2:65–9.

Cajochen C, Knoblauch V, Kräuchi K, Renz C, Wirz-Justice A. Dynamics of frontal EEG activity, sleepiness and body temperature under high and low sleep pressure. NeuroReport 2001;12:2277–81.

De Gennaro L, Ferrara M, Bertini M. Effect of slow-wave sleep deprivation on topographical distribution of spindles. Behav Brain Res 2000a;116:55–9.

De Gennaro L, Ferrara M, Bertini M. Topographical distribution of spindles: variations between and within NREM sleep cycles. Sleep Res Online 2000b;3:155–60.

Dijk DJ, Beersma DGM, Daan S. EEG power density during nap sleep: reflection of an hourglass measuring the duration of prior wakefulness. J Biol Rhythms 1987;2:207–19.

Dijk DJ, Hayes B, Czeisler CA. Dynamics of electroencephalographic sleep spindles and slow wave activity in men: effect of sleep deprivation. Brain Res 1993;626:190–9.

Dijk DJ, Shanahan TL, Duffy JF, Ronda JM, Czeisler CA. Variation of electroencephalographic activity during non-rapid eye movement and rapid eye movement sleep with phase of circadian melatonin rhythm in humans. J Physiol 1997;505:851–8.

Finelli LA, Achermann P, Borbély AA. Individual 'fingerprints' in human sleep EEG topography. Neuropsychopharmacology 2001a;25:S57–S62.

Finelli LA, Borbély AA, Achermann P. Functional topography of the human nonREM sleep electroencephalogram. Eur J Neurosci 2001b;13(12):2282–90.

Gibbs FA, Gibbs EL. Atlas of electroencephalography, 2nd ed. Cambridge: Addison-Wesley Press; 1950.

Knoblauch V, Kräuchi K, Renz K, Wirz-Justice A, Cajochen C. Homeostatic control of slow-wave and spindle frequency activity during human sleep: effect of differential sleep pressure and brain topography. Cereb Cortex 2002;12:1092–100.

Knoblauch V, Wirz-Justice A, Kräuchi K, Cajochen C. Regional differences in the circadian modulation of human sleep spindle characteristics. Eur J Neurosci 2003;18:155–63.

Martens WLJ. The fast time frequency transform (F.T.F.T.): a novel on-line approach to the instantaneous spectrum. 14th International Conference of the IEEE Engineering in Medicine and Biology Society, Paris; 1992.

Martens WLJ. Segmentation of 'rhythmic' and 'noisy' components of sleep EEG, heart rate and respiratory signals based on instantaneous amplitude, frequency, bandwidth and phase. 1st Joint BMES/EMBS IEEE Conference, Atlanta; 1999.

Nuñez A, Curro Dossi R, Contreras D, Steriade M. Intracellular evidence for incompatibility between spindle and delta oscillations in thalamocortical neurons of cat. Neuroscience 1992;48:75–85.

Pivik RT, Harman K. A reconceptualization of EEG alpha activity as an index of arousal during sleep: all alpha activity is not equal. J Sleep Res 1995;4:131–7.

Rechtschaffen A, Kales A. A manual of standardized terminology, techniques and scoring system for sleep stages of human subjects. Bethesda, MD: US Department of Health, Education and Welfare, Public Health Service; 1968.

Scheuler W, Kubicki S, Scholz G, Marquardt J. Two different activities in the sleep spindle frequency band-discrimination based on the topographical distribution of spectral power and coherence. Sleep 1990;90:13–16.

Sejnowski TJ, Destexhe A. Why do we sleep? Brain Res 2000;886: 208–23.

Steriade M, McCormick DA, Sejnowski TJ. Thalamocortical oscillations in the sleeping and aroused brain. Science 1993;262:679–85.

Trachsel L, Dijk DJ, Brunner DP, Klene C, Borbély AA. Effect of zopiclone and midazolam on sleep and EEG spectra in a phase-advanced sleep schedule. Neuropsychopharmacology 1990;3:11–18.

Uchida S, Maloney T, March JD, Azari R, Feinberg I. Sigma (12–15 Hz) and delta (0.3–3 Hz) EEG oscillate reciprocally within NREM sleep. Brain Res Bull 1991;27:93–6.

Werth E, Achermann P, Dijk DJ, Borbély AA. Spindle frequency activity in the sleep EEG: individual differences and topographic distribution. Electroenceph clin Neurophysiol 1997;103:535–42.

Zeitlhofer J, Gruber G, Anderer P, Asenbaum S, Schimicek P, Saletu B. Topographic distribution of sleep spindles in young healthy subjects. J Sleep Res 1997;6:149–55.

Zygierewicz J, Blinowska KJ, Durka PJ, Szelenberger W, Niemcewicz S, Androsiuk W. High resolution study of sleep spindles. Clin Neurophysiol 1999;110:2136–47.